



Bio-electrolytic sensor for rapid monitoring of volatile fatty acids in anaerobic digestion process

Jin, Xiangdan; Li, Xiaohu; Zhao, Nannan; Zhang, Yifeng; Angelidaki, Irini

Published in:
Water Research

Link to article, DOI:
[10.1016/j.watres.2016.12.045](https://doi.org/10.1016/j.watres.2016.12.045)

Publication date:
2017

Document Version
Peer reviewed version

[Link back to DTU Orbit](#)

Citation (APA):
Jin, X., Li, X., Zhao, N., Zhang, Y., & Angelidaki, I. (2017). Bio-electrolytic sensor for rapid monitoring of volatile fatty acids in anaerobic digestion process. *Water Research*, 111, 74-80.
<https://doi.org/10.1016/j.watres.2016.12.045>

General rights

Copyright and moral rights for the publications made accessible in the public portal are retained by the authors and/or other copyright owners and it is a condition of accessing publications that users recognise and abide by the legal requirements associated with these rights.

- Users may download and print one copy of any publication from the public portal for the purpose of private study or research.
- You may not further distribute the material or use it for any profit-making activity or commercial gain
- You may freely distribute the URL identifying the publication in the public portal

If you believe that this document breaches copyright please contact us providing details, and we will remove access to the work immediately and investigate your claim.

16 **Abstract**

17 This study presents an innovative biosensor that was developed on the basis of a microbial electrolysis
18 cell for fast and reliable measurement of volatile fatty acids (VFA) during anaerobic digestion (AD)
19 process. The bio-electrolytic sensor was first tested with synthetic wastewater containing varying
20 concentrations of VFA. A linear correlation ($R^2=0.99$) between current densities (0.03 ± 0.01 to
21 2.43 ± 0.12 A/m²) and VFA concentrations (5-100 mM) was found. The sensor performance was then
22 investigated under different affecting parameters such as the external voltage, VFA composition ratio,
23 and ionic strength. Linear relationship between the current density and VFA concentrations was always
24 observed. Furthermore, the bio-electrolytic sensor proved ability to handle interruptions such as the
25 presence of complex organic matter, anode exposure to oxygen and low pH. Finally, the sensor was
26 applied to monitor VFA concentrations in a lab-scale AD reactor for a month. The VFA measurements
27 from the sensor correlated well with those from GC analysis which proved the accuracy of the system.
28 Since hydrogen was produced in the cathode as byproduct during monitoring, the system could be
29 energy self-sufficient. Considering the high accuracy, short response time, long-term stability and
30 additional benefit of H₂ production, this bio-electrolytic sensor could be a simple and cost-effective
31 method for VFA monitoring during AD and other anaerobic processes.

32 **Keyword:** Volatile fatty acid; Biosensor; Microbial electrolysis cell; Anaerobic digestion; Hydrogen

33

34

35 **1. Introduction**

36 Biogas, an alternative to fossil fuels, is becoming a promising source of renewable energy
37 worldwide. In Europe, there are more than 14500 biogas plants by 2014 with total installed capacity of
38 7857 MWel (Dahlin et al., 2015). However, process instability caused by clogging, foaming and
39 ammonia inhibition is often encountered in anaerobic digestion (AD), which may cause serious
40 economic losses and prevent this technology from being widely applied. To prevent such problem and
41 to ensure the biogas unit a long life-span, monitoring of the AD process is crucial. Parameters like
42 volatile fatty acid (VFA) concentrations, pH, biogas yield, biogas composition and alkalinity are
43 commonly used as indicators of the complex biochemical process (Li et al., 2014). Among those
44 indicators, it is widely acknowledged that the concentration of VFAs in the digester is prone to be a
45 more meaningful indicator of the process status (Falk et al., 2015). Several off-line methods for VFA
46 monitoring such as titration method (Purser et al., 2014), GC (Boe et al., 2007), high performance
47 liquid chromatography (HPLC) and mid-infrared spectroscopy (Falk et al., 2015) have been developed.
48 However, these methods are time consuming, inaccurate, expensive and typically tested manually.
49 There are also a few online VFA monitoring systems based on the aforementioned methods (Boe and
50 Angelidaki, 2012). Nevertheless, those systems often require complex equipment and careful
51 maintenance, or need difficult sample preparation, which prevents their widely application. Therefore,
52 development of an efficient, accurate and cost-effective VFA sensing system is crucial for the
53 application of AD technology.

54 In recent years, bioelectrochemical systems (BESs) have demonstrated great potential to be
55 alternatives for water quality measurement. In particular, microbial fuel cell, a typical BES, has been
56 applied as biosensors for monitoring biochemical oxygen demand (BOD) (Zhang and Angelidaki,

57 2011), dissolved oxygen (DO) (Zhang and Angelidaki, 2012), microbial activity (Zhang and
58 Angelidaki, 2011), toxic components (Shen et al., 2013; Jiang et al., 2015), and even VFA
59 concentrations (Kaur et al., 2013). BES-based biosensors have attracted great attention due to the
60 advantages of cost-effective, rapid, sustainable and portable. The first demonstration of VFAs
61 quantitative measurement in a MFC was presented by Kaur et al (2013). They further modified the
62 anode by the immobilization of bacteria to ensure the sensor's stability and repeatability (Kaur et al.,
63 2014). However, the detection range is quite limited for real application which is less than 80 mg/L and
64 it would still function as a sensor of total organic matter instead of VFAs with real wastewater. To
65 solve these problems, a VFA biosensor based on the principle of a microbial desalination cell (MDC)
66 was proposed by our group which could detect a wide range of VFAs and eliminate the effect of
67 sample matrix and complex organic matter (Jin et al., 2016). Nevertheless, the response time of the
68 sensor could be shortened as well as the complex three-chambered architecture could be simplified
69 further.

70 In this study, an innovative biosensor based on a microbial electrolysis cell (MEC) was developed
71 to monitor VFA concentrations during AD process. The bio-electrolytic sensor was constituted of only
72 two chambers and the synthetic wastewater was dosed into the cathode chamber. An external voltage
73 was supplied to accelerate the transportation of VFAs from the cathode to anode through an anion
74 exchange membrane (AEM). With such system, the response time and capital cost could be greatly
75 reduced compared to those of the previous MDC-based VFA sensor. Furthermore, H₂ could be
76 produced at the cathode during the monitoring activity, which may partly compensate the energy used
77 for powering the sensor. The aim of the present study is to provide proof-of-concept evidence that the
78 bio-electrolytic sensor can be an alternative to the traditional complex and time-consuming analytical
79 methods for the real-time detection of VFA concentrations in anaerobic process. With this purpose, the

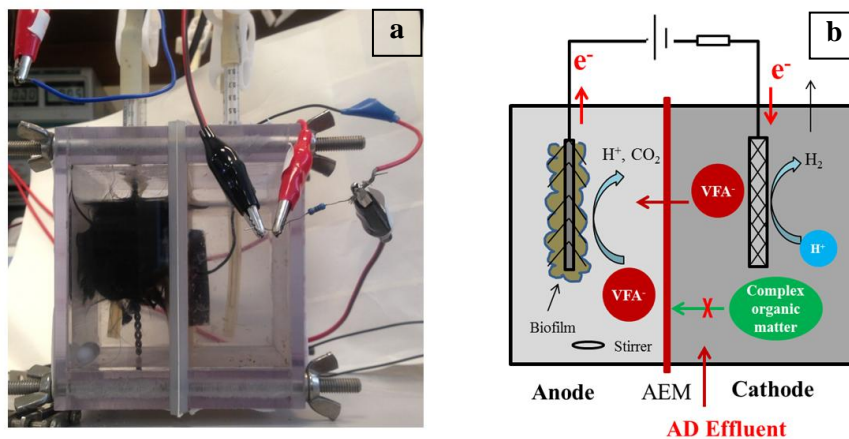
80 current response of bio-electrolytic sensor to various VFA concentrations in the artificial wastewater
81 (mimicking AD effluent) was tested in terms of response time, detection range, sensitivity and
82 operational stability. The effect of external voltage, VFA composition, and ionic strength on the
83 performance of the sensor was investigated. The interference such as the presence of complex organic
84 matter, anode exposure to oxygen and the effect of low pH on the system performance was explored.
85 Finally, effluent from a lab-scale AD reactor fed with manure and industrial food-wastes was detected
86 by the bio-electrolytic sensor for 30 days to verify the sensor's reliability. The application of the bio-
87 electrolytic sensor might have the potential to supply an efficient way to control AD process and bring
88 economic benefit.

89 **2. Material and methods**

90 2.1. Biosensor Setup and Operation

91 Two double-chamber reactors constructed of nonconductive polycarbonate plates were used in this
92 study. The dimensions of the anode and cathode chambers were the same (8×8×4 cm) for both reactors.
93 Anion exchange membrane (AEM) (AMI 7001, Membrane international, NJ, 9×9 cm) was used to
94 separate the two chambers. Prior to use, membranes were soaked overnight in 50 M NaCl solution, and
95 then stored in distilled water until placed in the cell. The reactors were tightened by rubber gaskets and
96 screws to avoid leakage. The anode electrode was made of carbon brush (5.0 cm in diameter, 5.0 cm in
97 length, Mill-Rose, USA) and was attached with biofilm since it was obtained from an existing
98 microbial electrochemical system (Jin et al., 2016). The cathode electrode was a titanium woven wire
99 mesh (4×5 cm, 0.15 mm aperture, William Gregor Limited, London) coated with 0.5 mg/cm² Pt.
100 Rubber tubes were inserted for medium refill and gas collection. A power supply (HQ PS3003,

101 Helmholtz Elektronik A/S, Denmark) was used to provide an additional voltage to the circuit. The
102 positive lead of the power source was connected to the anode electrode, and the negative lead was
103 connected to a 10 Ω resistance connecting the cathode electrode in the circuit (Fig. 1).



104

105 **Fig. 1.** Prototype (a) and schematic diagram (b) of the bio-electrolytic sensor.

106 The anode electrode was initially operated in the MFC mode without substrates for several days
107 until the current density decreased below 0.1 A/m². During the experiment, the anode chamber was
108 filled with approximately 220 mL of buffer solution (pH = 7.22±0.17) containing 50 mM phosphate
109 buffer (Na₂HPO₄, 4.33 g/L; and NaH₂PO₄, 2.03 g/L) and nutrient solution (NH₄Cl, 0.31 g/L; KCl, 0.13
110 g/L; 12.5 mL mineral solution and 12.5 mL vitamin solution) (Kvesitadze et al., 2012). The cathode
111 was filled with 220 mL of synthetic wastewater as “artificial AD effluent”, which was prepared with
112 the same buffer solution containing varying concentrations of sodium acetate, sodium propionate and
113 sodium butyrate (total VFAs ranges from 0 to 120 mM). To mimic real AD effluent, we set the
114 concentration ratio of acetate, propionate and butyrate in “artificial AD effluent” at 5:1:1 which
115 corresponds well to what is often measured in biogas plants (Hollinshead et al., 2014). In one set of
116 tests, we tested the sensor with voltages at 0.3, 0.5, 0.8 and 1.0 V to elucidate the effect of external
117 voltage on the current generation. Then the effect of VFA composition on the system was studied: at

118 three different concentration ratios (acetate: propionate: butyrate were 5: 1: 1 (R_1), 10: 10: 1 (R_2), and
119 20: 5: 1 (R_3)). Subsequently the performance of the system was evaluated under different ionic strength
120 by adding 0, 20, 40, and 80 mM NaCl to the artificial AD effluent. Both chambers were purged with N_2
121 for 15 min to maintain anaerobic conditions prior to each batch run. Mixing was ensured in the anode
122 by a magnetic stirrer. A gas bag was connected with the cathode to collect the produced hydrogen. All
123 chemicals were of reagent grade. All experiments were carried out in duplicate at least at room
124 temperature ($22\pm 2^\circ C$).

125 2.2. Electrochemical Analyses and Calculations

126 Conductivity and pH were measured by a CDM 83 conductivity meter (Radiometer) and a PHM
127 210 pH meter (Radiometer), respectively. VFAs were measured using a GC with FID detection
128 (Agilent 6890). Hydrogen was analyzed by a GC-TCD fitted with a 4.5 m \times 3 mm s-m stainless column
129 packed with Molsieve SA (10/80). Voltage readings were taken every 10 mins using a digital
130 multimeter (Model 2700, Keithley Instruments, Inc.; Cleveland, OH, USA). Current density was
131 calculated as $i=I/A$, where I (A) is the current calculated according to ohm's law and A (m^2) is the
132 project surface area of the cathode. The amount of energy supplied to the sensor by the power source
133 (W_E) and the energy efficiency (η_E) relative to the electricity input were calculated as below:

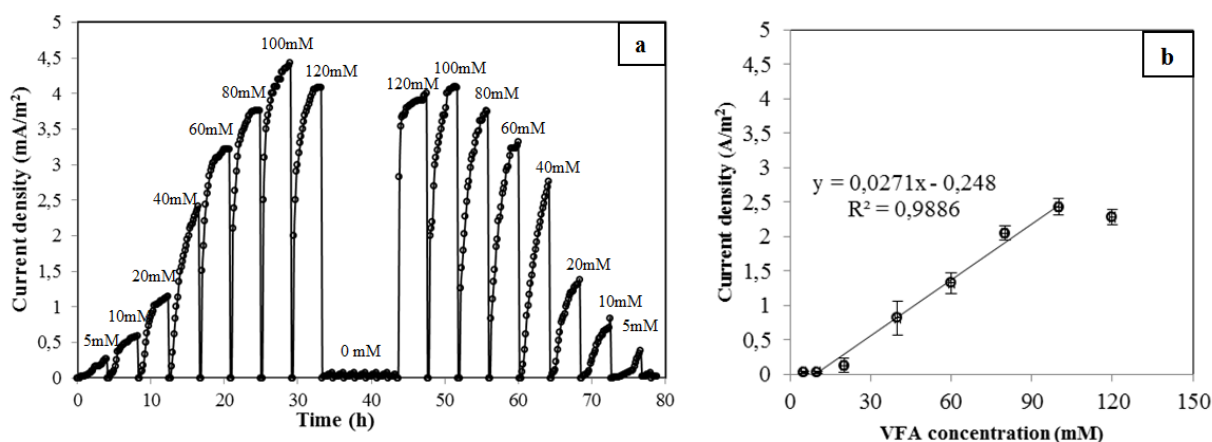
$$134 W_E = \sum_1^n (IE \Delta t)$$

$$135 \eta_E = \frac{n_{H_2} \Delta H_{H_2}}{W_E}$$

136 Where E (V) is the voltage applied to the sensor, Δt (s) is the time increment for n data points
137 measured during the experiment, n_{H_2} is the number of moles of hydrogen collected during operation,
138 ΔH_{H_2} (285.83 kJ/mol) is the energy content of hydrogen based on the heat combustion.

139 3. Results and Discussion

140 3.1. The Response of the Bio-electrolytic Sensor to Variations of VFA Concentrations



141

142 **Fig. 2.** Typical current density generation along with time from the biosensor (a) and the relationship between
143 current density generated at 1 h and initial VFA levels in the artificial AD effluent (b).

144 The feasibility of the bio-electrolytic sensor was demonstrated with the artificial AD effluent at
145 VFA concentrations ranging from 5 to 120 mM. Fig. 2a shows the current output along with time under
146 varied VFA levels. The external voltage was 0.5 V and the concentration ratio of acetate, propionate
147 and butyrate was 5:1:1. At each VFA concentration, it was found that the current density increased
148 along with the time and reached to a platform within 4 hours. No significant increase was observed
149 thereafter (data was not shown). It could be due to the establishment of equilibrium between VFA
150 transportation from the cathode to anode chamber and VFA microbial consumption by anodic bacteria.

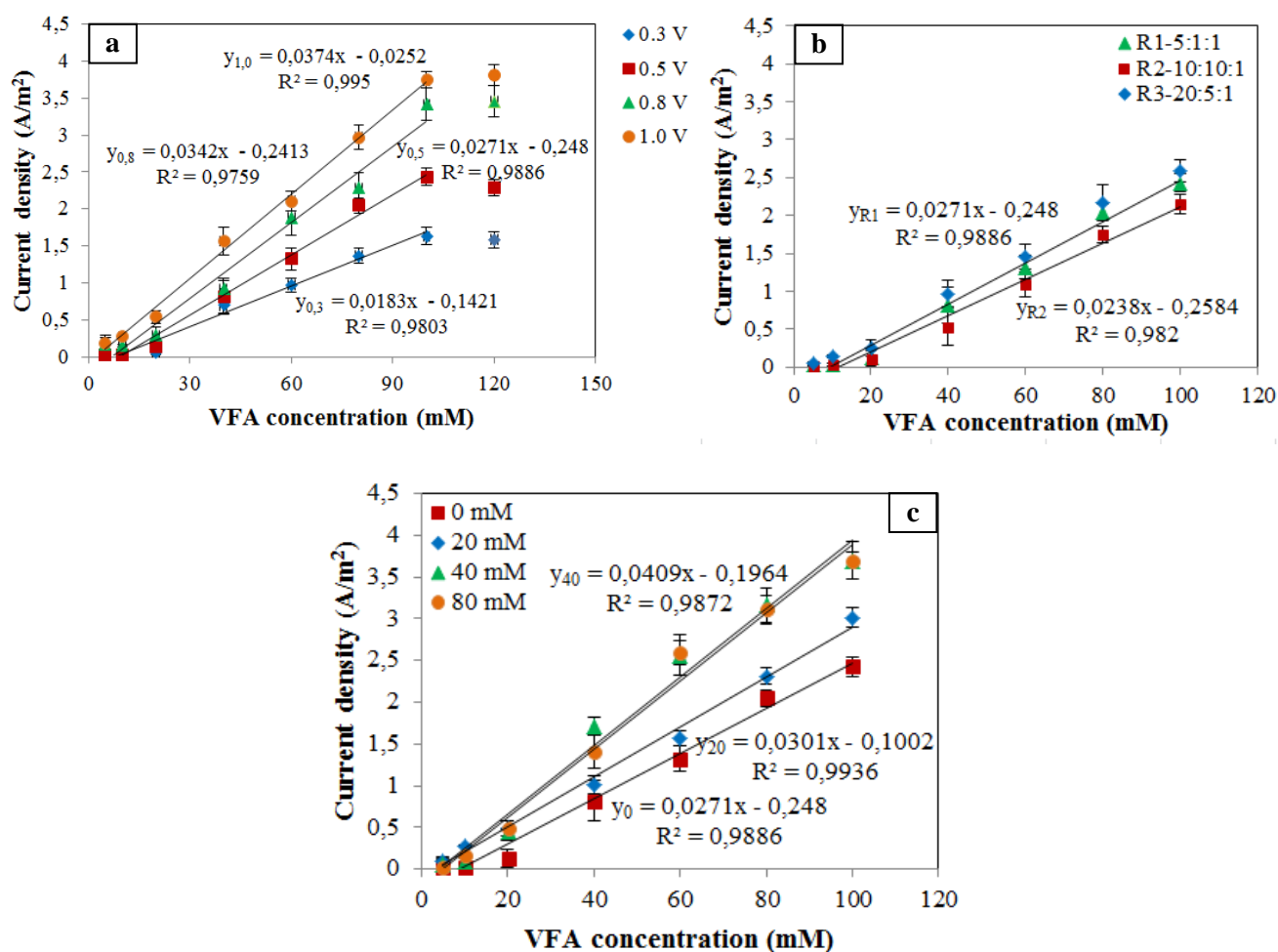
151 Therefore, the reaction time of the sensor was chosen as 4 h for each sample in the following tests.
152 When organic matter was omitted from the artificial AD effluent in the cathode, the current density was
153 as low as observed during the starvation period ($<0.1 \text{ A/m}^2$, 0 mM VFA). It was observed that the
154 maximum current density increased with VFA concentrations and vice versa within a certain VFA
155 concentration range (5~100 mM). As indicated in Fig. 2a, the sensor showed a good reproducibility
156 independently the sequence of measurements and was not affected by VFA concentrations changed
157 from low to high or oppositely. Furthermore, the sensor recovered immediately after a period of
158 starvation and functioned well as soon as VFA were introduced into the sensor.

159 As shown in Fig. 2b, current densities obtained at 1 h were plotted as the function of initial VFA
160 concentrations. The current density increased from 0.03 ± 0.01 to $2.43 \pm 0.12 \text{ A/m}^2$ with VFA
161 concentrations increasing from 5 to 100 mM. A linear relationship was obtained with a high correlation
162 coefficient factor ($R^2 > 0.98$). No additional increase in the current output was observed when VFA
163 concentrations were above 100 mM, which suggests that the current density was saturated at higher
164 VFA concentrations. The current density obtained at 2, 3 or 4 h also showed linear relationship with
165 VFA concentration (Fig. S1-3, Supplementary data). Since a relatively short response time was wished,
166 current densities generated at 1 h were focused in the subsequent tests. The results above clear
167 demonstrated the applicability of the sensor for VFA monitoring. The detection range of the bio-
168 electrolytic sensor was up to 100 mM which is much higher than that of MFC-based sensor (Kaur et al.,
169 2013) and almost at the same level as that of the MDC-based sensor reported previously (Jin et al.,
170 2016). It should be noted that the response time (i.e., 1 h) achieved in this study was much shorter
171 compared to that (5 h) of the previous MDC-based sensor. The response of the current density to VFAs
172 in the cathode suggested that VFAs first transported through the AEM and then were utilized by the
173 anodic exoelectrogenic biofilm. Migration and diffusion could be the main mechanisms responsible for

174 such transportation, and thus, the relatively quicker response time could be due to the enhanced
 175 migration with external voltage supply (discussed later).

176 3.2. Sensor Performance under Different Operational Conditions

177 A series of experiments were conducted to study the individual effect of external voltage, VFA
 178 composition ratio, and solution ionic strength on the sensor performance.



179

180

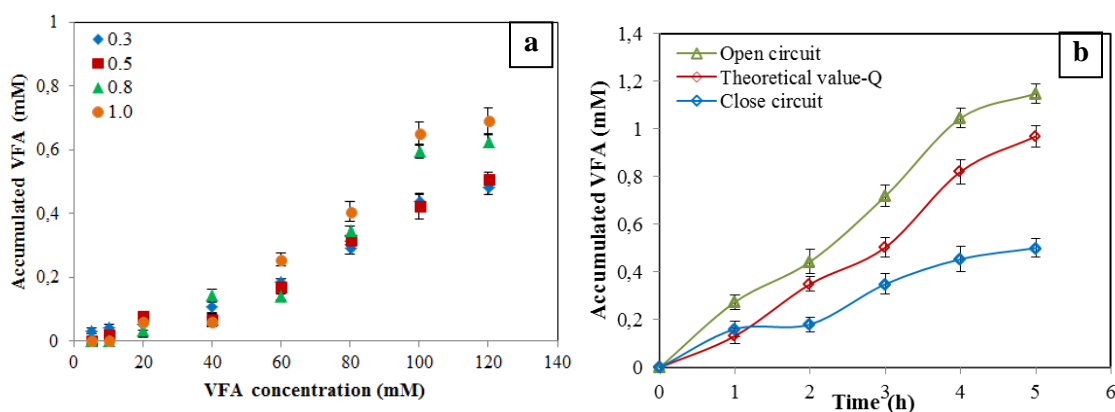
181 **Fig. 3.** Current densities against VFA levels under different external voltage (a), initial VFA concentration ratios
 182 (b), and ionic strength with NaCl (c).

183 Fig. 3a shows the current density generated at 1 h along with varied VFA concentrations under
184 different external voltage. The linear relationships between current densities (0.02 ± 0.01 to 1.63 ± 0.12
185 A/m^2 at 0.3 V; 0.03 ± 0.01 to 2.43 ± 0.12 A/m^2 at 0.5 V; 0.15 ± 0.05 to 3.42 ± 0.21 A/m^2 at 0.8 V; 0.19 ± 0.07
186 to 3.74 ± 0.11 A/m^2 at 1.0 V) and VFA concentrations (5-100 mM) were observed at all the external
187 voltages. Furthermore, the current density increased with the increasing external voltage. It was also
188 found that the difference among the current densities observed with different external voltages was
189 much larger at high VFA concentrations than that at low VFA concentrations. For instance, with 100
190 mM VFA in the artificial AD effluent, the current density generated at 1.0 V was 3.74 ± 0.11 A/m^2 ,
191 which was much higher than that obtained at 0.3 V (1.63 ± 0.12 A/m^2). However, while the initial VFAs
192 were below 20 mM, the differences among the current densities under different voltages were not
193 significant. It is due to that the substrate was the main limiting factor at low VFA concentrations while
194 the external voltage turned to be dominant when sufficient substrate was supplied. The higher voltage
195 applied the faster VFA transportation to the anode, which might explain the increase of current density
196 with higher external voltage (discussed in later section). At the end of experiments, 14.0, 27.5, 34.0,
197 and 41.5 mL H_2 was collected at 0.3, 0.5, 0.8 and 1.0 V, respectively. The energy efficiencies related to
198 the electrical input were 137.6%, 158.6%, 103.3% and 120.8%, respectively. The result was
199 comparable to traditional MEC systems (Zhang and Angelidaki, 2014). Therefore, the bio-electrolytic
200 sensor could realize energy self-sufficient with H_2 production in addition to VFA monitoring. To
201 achieve the highest energy efficiency, 0.5 V was selected as external voltage in the following tests.

202 Acknowledging that VFA composition might influence the anion transportation across the AEM
203 and the anodic microbial communities as well as the sensor performance, the sensor was further tested
204 at three different VFA ratios (i.e., R_1 , R_2 and R_3) to address such concerns. The correlation between
205 current densities and VFA concentrations at different VFA composition is shown in Fig. 3b. Similar

206 results were obtained at R_1 and R_3 , and the regression function was still suitable. Comparatively,
207 relatively lower current density was observed at R_2 resulting in a slightly decrease of the slope of the
208 linear function. It has been recently reported that the transportation rate of acetate was faster than those
209 of propionate and butyrate through the AEM which can be anticipated due to the smaller molecule size
210 of acetate (Zhang and Angelidaki, 2015). Moreover, propionate and butyrate degradations have been
211 known to be thermodynamically less favorable as compared to acetate degradation (Yang et al., 2015).
212 The proportion of acetate (>70%) was much higher than the proportions of propionate and butyrate at
213 R_1 and R_3 while the proportion of acetate (<50%) was smaller at R_2 , which might cause the decrease in
214 current density at R_2 . Since the amount of acetate was always dominant in real AD effluent, the bio-
215 electrolytic sensor is practicable in field application.

216 Subsequently our system was examined as a function of the ionic strength. Thus NaCl were added
217 in the artificial AD effluent to study their impact on the sensor performance. Results are shown in Fig.
218 3c. The current density still displayed linear relationship with VFA levels at different ionic strengths.
219 The current density generally increased with the increasing ionic strength, resulting in the change of the
220 regression function. For example, by increasing the solution ionic strength from 20 to 40 mM with
221 NaCl, the current density obtained at 100 mM VFA increased from 3.01 ± 0.11 to 3.70 ± 0.15 A/m². This
222 could be due to the decrease of the internal resistance as result of the conductivity elevation (Fig. S4,
223 Supplementary data) at high ionic strength. However, the current density ceased to increase when the
224 NaCl concentration was higher than 40 mM, indicating the saturation of current density at this ionic
225 strength level (Liu et al., 2005). Since the ionic strength in real AD effluent was usually higher than 80
226 mM (Cai et al., 2013; Sheets et al., 2014), the results from the system will be still valid. However, in
227 practical applications the sensor may need calibration by taking practical environmental conditions into
228 account such as wastewater was diluted.



229

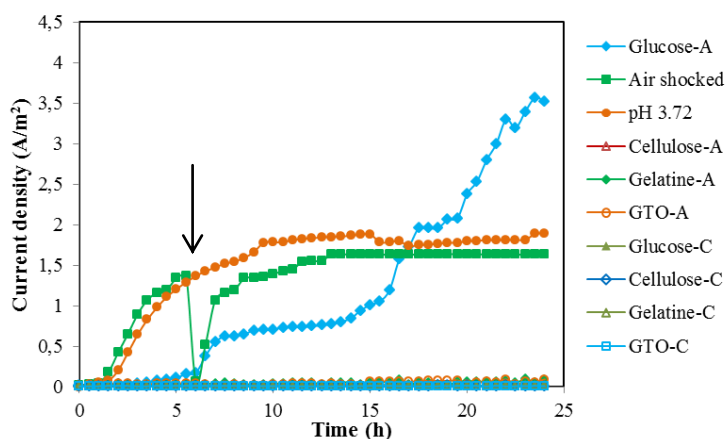
230 **Fig. 4.** Accumulated VFAs in the anode chamber at 1 h under different external voltage (a); Accumulated VFAs
 231 in the anode under different conditions: open circuit; close circuit and theoretical value calculated by the
 232 accumulated charge (b).

233 3.3. Mechanism of VFA transportation

234 The accumulated VFA concentration in the anode under different voltage was measured (Fig. 4a). It
 235 was indeed observed that higher voltage caused more VFA to accumulate in the anode under the same
 236 initial VFA concentration which is the dosed VFAs in the cathode at the beginning of each batch. Such
 237 observation was even clear when the initial VFA concentration was higher than 40 mM. Interestingly,
 238 at same applied voltage, the accumulated VFA concentration in the anode increased with the initial
 239 VFA concentration of the artificial AD effluent. The results imply that besides electricity driven
 240 migration, diffusion caused by concentration gradient might also be responsible for VFA transportation.
 241 Then the accumulated VFA in the anode was monitored under both open circuit and closed circuit
 242 ($E=0.5$ V) along with the operation time when the initial VFA in the artificial AD effluent was 60 mM
 243 (Fig. 4b). VFA accumulation under open circuit confirmed the contribution of diffusion to the VFA
 244 transportation. Theoretically, most charge should be balanced by negative VFA ions migrating from the
 245 cathode to the anode chamber. Thus, the contribution of migration to the VFA transportation could be
 246 estimated on the basis of the accumulated charge (Q) during the monitoring. Notably, the actual

247 concentration of the accumulated VFA in the anode was much lower than that under open circuit or
248 calculated according to the accumulated charge, which implied the substrate consumption by the anodic
249 exoelectrogenic biofilm. In addition, it was noticed that the accumulated VFA concentration in the
250 anode under close circuit did not increase further after 4 h, indicating a dynamic equilibrium between
251 VFA consumption and transportation. This was consistent with the current density where a platform
252 was reached around 4 h.

253 3.4. Sensor performance under different interference situation



254

255 **Fig. 5.** Current density generation when organic matter was dosed in the cathode and anode, respectively; arrow
256 indicates when air sparging was applied; pH of the cathode solution was adjusted to 3.72.

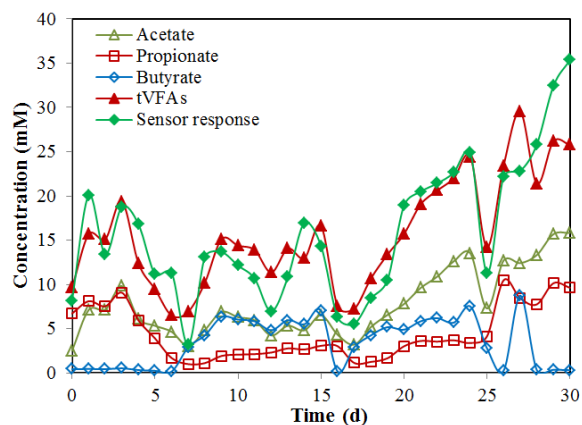
257 It is of utmost importance for a sensor to be robust to interruptions. Fig. 5 shows the response of
258 the sensor to different interferences. To test the selectivity of the sensor, we dosed a mixture of organic
259 matter (e.g., glucose, cellulose, protein and lipid) instead of VFAs into the cathode or anode chamber,
260 respectively. When 2 g/L glucose was added in the anode, stepwise increases in current density were
261 obtained. On the contrary, only background current density was observed when glucose was added into

262 the cathode as sole organic matter. As glucose is nonionic it was retained by the AEM in the same
263 chamber where it was added. Likewise, 2 g/L cellulose, 2 g/L gelation or 10 mL/L GTO in the cathode
264 didn't increase the current density. Comparatively, when some of them were dosed in the anode, very
265 low level of current density was observed since microorganisms may need a bit adaption time to
266 hydrolyze polymer into simple molecules. The results demonstrate the good selectivity of the bio-
267 electrolytic sensor, since the interference from complex organic matter could be avoided as the AD
268 effluent was fed into the cathode. It is one of the important advantages of the sensor developed in our
269 study compared to the previous MFC sensor in which the AD effluent is added into the anode chamber
270 (Kaur et al., 2013). Moreover, the sensor is able to detect a wide range of VFAs since only part of bulk
271 VFAs in the cathode transferred to the anodic biofilm. For assessing the recovery ability after a
272 possible disturbance, 12 mL air was injected to the anode using a syringe and the response of the sensor
273 was recorded. As shown in Fig. 5, anodic biofilm reacted immediately to air pulses by ceasing
274 electricity generation. After 1 hour the current density generation resumed which underlined the
275 resilience of the sensor. Subsequently, we investigated the sensor performance at low pH condition by
276 adjusting the pH of artificial AD effluent to 3.72. Results showed that the sensor performance was not
277 influenced by the low pH as proton transportation towards to anode was prevented by the AEM.
278 Therefore, the utilization of AEM and dosing artificial AD effluent in the cathode made the system
279 selective and robust.

280 3.5. Verification of the sensor with effluents from real AD reactor

281 The sensor was finally applied to measure VFA levels in a real lab-scale CSTR. During 30 days
282 operation of the CSTR, samples were retrieved from the reactor every day and immediately dosed into

283 the cathode of the bio-electrolytic sensor for measurement. The operational data for the CSTR and
284 characteristics of the effluent are listed in Table S1 (Supplementary data). VFA concentrations obtained
285 from our sensor and GC are summarized in Fig. 6. The fluctuation in VFA levels was observed through
286 the sensor with good sensitivity. The values obtained with the sensor agreed well with the total VFA
287 values measured by GC. ANOVA analysis detected no significant difference between the two groups
288 ($F=0.54 > F_{(30, 29)}=0.11$, $P \leq 0.05$), which confirmed the good accuracy of the sensor. According to the
289 results, the sensor can easily handle samples from AD reactors with a wide range of VFA levels.
290 Especially, the sensor concept is simple which makes it potentially applicable to various anaerobic
291 processes. Furthermore, this bio-electrolytic sensor has been operated over 5 months in a stable manner
292 without any maintenance service, which demonstrates the reliability of the sensor system.



293
294 **Fig. 6.** Monitoring test of a lab-scale CSTR.

295 4. Conclusion

296 The present work demonstrated for the first time the feasibility of the MEC-typed sensor for VFA
297 monitoring in AD process. Reproducible current densities as a function of different VFA
298 concentrations over a wide range (0-100 mM) were obtained. The external voltage, VFA composition
299 and ionic strength affected the sensor performance. Nevertheless linear relationships between current

300 density and VFA levels were always observed. The sensor had a high selectivity since complex organic
301 matter was retained by AEM which only allowed VFA transport through. Moreover it was robust to
302 interruptions such as low pH and resumed soon after expose to air. Hydrogen was produced during the
303 measurement which could compensate (or partly) the energy requirements of the sensor. Though the
304 bio-electrolytic sensor has a potential in monitoring biogas process, further improvements and
305 modifications such as more compact sensor and robust structure is necessary to fit the onsite and real
306 time monitoring.

307 **Acknowledgement**

308 The authors would like to acknowledge China Scholarship Council for the financial support. The
309 authors thank the technical assistance by Hector Gracia with analytical measurements and Viviana
310 Negro for supplying AD effluents from her AD reactor. This research is supported financially by the
311 Danish Council for Independent Research (DFF-1335-00142).

312 **References**

- 313 Boe, K., Batstone, D.J., Angelidaki, I., 2007. An innovative online VFA monitoring system for the
314 anaerobic process, based on headspace gas chromatography. *Biotechnol. Bioeng.* 96(4), 712- 721.
- 315 Boe, K., Angelidaki, I., 2012. Pilot-scale application of an online VFA sensor for monitoring and
316 control of a manure digester. *Water Sci. Technol.* 66(11), 2496-2503.
- 317 Cai, T., Park, S.Y., Racharaks, R., Li, Y., 2013. Cultivation of *Nannochloropsis salina* using anaerobic
318 digestion effluent as a nutrient source for biofuel production. *Appl. Energy.* 108, 486-492.

319 Dahlin, J., Herbes, C., Nelles, M., 2015. Biogas digestate marketing: Qualitative insights into the
320 supply side. *Conservation Recycl.* 104, 152-161.

321 Falk, H.M., Reichling, P., Andersen, C., Benz, R., 2015. Online monitoring of concentration and
322 dynamics of volatile fatty acids in anaerobic digestion processes with mid-infrared spectroscopy.
323 *Bioprocess Biosyst. Eng.* 38(2), 237-249.

324 Hollinshead, W.D., Varman, A.M., You, L., Hembree, Z., Tang, Y.J., 2014. Boosting d-lactate
325 production in engineered cyanobacteria using sterilized anaerobic digestion effluents. *Bioresour.*
326 *Technol.* 169, 462-467.

327 Jiang, Y., Liang, P., Zhang, C., Bian, Y., Yang, X., Huang, X., Girguis, P.R., 2015. Enhancing the
328 response of microbial fuel cell based toxicity sensors to Cu(II) with the applying of flow-
329 through electrodes and controlled anode potentials. *Bioresour. Technol.* 190, 367-372.

330 Jin, X., Angelidaki, I., Zhang, Y., 2016. Microbial electrochemical monitoring of volatile fatty acids
331 during anaerobic digestion. *Environ. Sci. Technol.* 50 (8), 4422–4429.

332 Kaur, A., Kim, J.R., Michie, I., Dinsdale, R.M., Guwy, A.J., Premier, G.C., 2013. Microbial fuel cell
333 type biosensor for specific volatile fatty acids using acclimated bacterial communities. *Biosens.*
334 *Bioelectron.* 47, 50-55.

335 Kaur, A., Ibrahim, S., Pickett, C.J., Michie, I.S., Dinsdale, R.M., Guwy, A.J., Premier, G.C., 2014.
336 Anode modification to improve the performance of a microbial fuel cell volatile fatty acid
337 biosensor. *Sens. Actuators, B* 201, 266-273.

338 Kvesitadze, G., Sadunishvili, T., Dudaauri, T., Zahariashvili, N., Partskhaladze, G., Ugrekhelidze, V.,
339 Tsiklauri, G., Metreveli, B., Jobava, M., 2012. Two-stage anaerobic process for bio-hydrogen
340 and bio-methane combined production from biodegradable solid wastes. *Energy.* 37(1), 94-102.

341 Li, L., He, Q., Wei, Y., He, Q., Peng, X., 2014. Early warning indicators for monitoring the process
342 failure of anaerobic digestion system of food waste. *Bioresour. Technol.* 171, 491-494.

343 Liu, H., Cheng, S., Logan, B.E., 2005. Power Generation in Fed-Batch Microbial fuel cells as a
344 function of ionic strength, temperature, and reactor configuration. *Environ. Sci. Technol.* 39(14),
345 5488-5493.

346 Purser, B.J., Thai, S.-M., Fritz, T., Esteves, S., Dinsdale, R., Guwy, A., 2014. An improved titration
347 model reducing over estimation of total volatile fatty acids in anaerobic digestion of energy
348 crop, animal slurry and food waste. *Water Res.* 61, 162-170.

349 Sheets, J.P., Ge, X., Park, S.Y., Li, Y., 2014. Effect of outdoor conditions on *Nannochloropsis salina*
350 cultivation in artificial seawater using nutrients from anaerobic digestion effluent. *Bioresour.*
351 *Technol.* 152, 154-161.

352 Shen, Y., Wang, M., Chang, I.S., Ng, H.Y., 2013. Effect of shear rate on the response of microbial fuel
353 cell toxicity sensor to Cu(II). *Bioresour. Technol.* 136, 707-710.

354 Yang, N., Hafez, H., Nakhla, G., 2015. Impact of volatile fatty acids on microbial electrolysis cell
355 performance. *Bioresour. Technol.* 193, 449-455.

356 Zhang, Y., Angelidaki, I., 2011. Submersible microbial fuel cell sensor for monitoring microbial
357 activity and BOD in groundwater: focusing on impact of anodic biofilm on sensor applicability.
358 *Biotechnol. Bioeng.* 108(10), 2339-2347.

359 Zhang, Y., Angelidaki, I., 2012. A simple and rapid method for monitoring dissolved oxygen in water
360 with a submersible microbial fuel cell (SBMFC). *Biosens. Bioelectron.* 38(1), 189-194.

361 Zhang, Y., Angelidaki, I., 2014. Microbial electrolysis cells turning to be versatile technology: Recent
362 advances and future challenges. *Water Res.* 56(1), 11-25.

363 Zhang, Y., Angelidaki, I., 2015. Bioelectrochemical recovery of waste-derived volatile fatty acids and
364 production of hydrogen and alkali. *Water Res.* 81, 188-195.

365

Electronic Supplementary Material (for online publication only)

[Click here to download Electronic Supplementary Material \(for online publication only\): Supplementary data.docx](#)